Available online at www.sciencedirect.com
ScienceDirect
Procedia Engineering 2 (2010) 203–212
Procedia Engineering
www.elsevier.com/locate/procedia

Fatigue 2010

Material model for finite element modelling of fatigue crack growth in concrete

Pryl Dobromil*, Cervenka Jan, Pukl Radomir

Cervenka Consulting, Na Hrebenkach 44, 150 00 Praha 5, Czech Republic

Received 8 March 2010; revised 11 March 2010; accepted 15 March 2010

Abstract

Although fatigue damage of concrete is an important problem in structures subjected to cyclic loading, there are not many high-cycle fatigue models available for use in conjunction with advanced concrete material models and nonlinear finite element analysis. The available models that are published in the literature (for instance [1]) usually deal with the low cycled fatigue when it is necessary to perform the numerical nonlinear analysis for all investigated cycles. This approach is definitely not applicable when it comes to high-cycle fatigue when it is usually necessary to consider millions of cycles. The available models (for instance [2]) for high-cycled fatigue are based on linear elastic fracture mechanics considerations and they are not readily applicable to the finite element analysis using the smeared crack approach.

The three-dimensional fracture-plastic model [3] in the finite element software ATENA has been extended to capture fatigue damage in tension (however, the model can be easily modified to also consider damage from compressive and tensile-compressive loads). The damage can result in new cracks or growth of existing ones.

To keep the material model as simple as possible, the implementation is based on a classical stress based model (S-N or Wöhler curve). The S-N criterion is translated into material damage, which is introduced into the material model on the basis of stress increments at each material point and the number of cycles. The S-N criterion is suitable to initiate damage into the intact material. However, in order to facilitate the necessary crack propagation and extension of a pre-existing damage an additional damage needs to be introduced. It is advantageous to base this damage not on stress cycles but rather on the cycles of crack opening displacements (delta COD). The paper will present the formulation of the new model for the high-cycle fatigue in a form that is suitable for the smeared crack model formulation and the finite element analysis. The model behaviour will be documented on small theoretical examples as well as by comparison with experimental data.

Keywords: fatigue; concrete; tension; material model; crack growth; smeared crack; S-N curve; crack opening displacement; damage; Finite Element Method

* Corresponding author. Tel.: +420 220 610 018 ; fax: +420 220 612 227 *E-mail address*: dobromil.pryl@cervenka.cz .

1877-7058 © 2010 Published by Elsevier Ltd.
doi:10.1016/j.proeng.2010.03.022

1. Introduction

A model is presented for fatigue crack propagation within the framework of the finite element smeared crack analysis. This model has been initially developed for fatigue life predictions of railroad concrete sleepers. As such it mainly concentrates on modelling fatigue behaviour of concrete under tensile load. It has been implemented in the ATENA Finite Element software package [4]. The new fatigue material is based on the existing three-dimensional fracture-plastic material model [3].

Nomenclature

β_{fat}	material parameter determining the slope of the Wöhler (S-N) curve
ε_{fat}^{f}	fatigue damage in form of maximum fracturing strain (see also $\varepsilon_{\max}^{f}$)
$\varepsilon_{\max}^{f}$	maximum fracturing strain occurred in the material point history (corresponds to the max. COD)
ξ_{fat}	material parameter determining the damage based on cyclic crack opening and closing
σ_{bas}	stress level before the application of the cycling load
σ_{upp}	max. stress level reached in each load cycle
F_{stat}	peak static load
f_c	(initial) compressive strength
f_t	(initial) tensile strength
L_t	crack band size
N	number of load cycles to failure
n	number of load cycles applied
R	cycle asymmetry coefficient
$f_t(w)$	softening law function
$f_t^{-1}(\sigma)$	inverse of the softening law function
Δw	crack opening difference during each cycle (delta COD)
w_{bas}	crack opening displacement before the application of the cycling load
w_f	failure fracturing displacement (at the upper stress)
w_{fat}	fatigue fracturing displacement
w_{max}	fracturing displacement where the tensile strength reaches zero (end of the softening law)

2. Fatigue Damage Calculation

Fatigue damage can be physically interpreted as a gradual growth of micro-cracks due to the repeated loading. In the fracture-plastic material model [3], the crack growth is controlled by the internal parameter $\varepsilon_{\max}^{f}$, which

represents the maximal fracturing strain reached during the cracking process at each crack. This parameter is used to determine the current tensile strength at each material point using the crack band size L_t and the tensile softening law $f_t(w)$ as depicted in Fig. 1. This means that the current tensile strength is determined using the tensile softening law as:

$$\sigma_t = f_t(w_{\max}), \quad w = \varepsilon^f_{\max} L_t,$$

where σ_t represents the current tensile strength, $w_{\max}$ is the maximal crack opening reached during the loading process and L_t is the crack band size, which as based on the element size (see [3]). In the proposed model, the fatigue damage is modelled by increasing the fracturing strain $\varepsilon^f_{\max}$ by two fatigue contributions. A contribution based on cycling stress controlled by the additional material parameter β_{fat}, and the contribution from crack opening and closing in each cycle, controlled by the material parameter ξ_{fat}. The former is dominant before cracking occurs, the latter in already cracked material. This means that the maximal fracturing strain is composed of the following contributions:

$$\varepsilon^f_{\max} = \varepsilon^s_{\max} + \varepsilon^\sigma_{fat} + \varepsilon^{COD}_{fat}$$

where $\varepsilon^s_{\max}$ is the maximal fracturing strain from static loading, ε^σ_{fat} is the additional fracturing strain from fatigue stress cycling and ε^{COD}_{fat} is the additional fracturing strain from the cycling crack opening.

2.1. Stress Based Contribution ε^σ_{fat}

The contribution from the cycling of tensile stresses is determined using a stress based model, that is based on the Wöhler curve:

$$\frac{\sigma_{upp}}{f} = 1 - \beta_{fat}(1-R)\log N, \qquad N = 10^{\left(\frac{1-\frac{\sigma_{upp}}{f}}{\beta_{fat}(1-R)}\right)},$$

where σ_{upp} stands for the maximum tensile or compression stress and f for the corresponding strength, f_t or f_c, $R = \frac{\sigma_{bas}}{\sigma_{upp}}$ is the coefficient of cycle asymmetry. Then, the contribution to the maximum fracturing strain $\varepsilon^f_{\max}$ in each principal direction is adjusted by adding

$$\varepsilon^\sigma_{fat} = \frac{w_{fat}}{L_t},$$

where $w_{fat} = \frac{n}{N} w_f$ and the failing crack opening displacement for the given stress $w_f = f_t^{-1}(\sigma_{upp})$ (see Fig. 1).

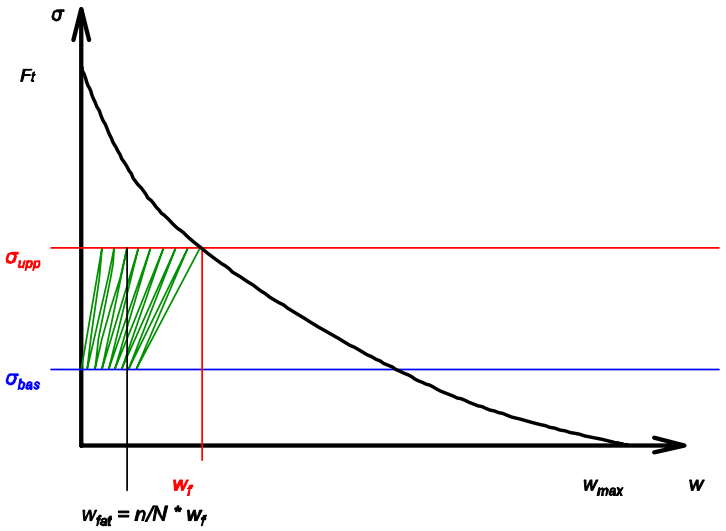

Fig. 1. Softening law and fatigue damage.

2.2. Crack Opening Based Contribution ε_{fat}^{COD}

The damage due to cracks that open and close during the cycling is determined as

$$\varepsilon_{fat}^{COD} = \frac{w_{fat}^{COD}}{L_t},$$

where $w_{fat}^{COD} = n\,\xi_{fat}\,\Delta w$, and Δw denotes the difference between the maximum and minimum crack opening during a cycle. The material parameter ξ_{fat} scales the damage contribution from cyclic crack opening and closing. The resulting ε_{fat}^{COD} is added to the maximal fracturing strain $\varepsilon_{\max}^{f}$ before the fatigue damage is introduced into the material.

2.3. Fatigue Damage Introduction

Several approaches of introducing the damage into the model were tested on the model. The additional fracturing strain due to fatigue, i.e. $\varepsilon_{fat}^{f} = \varepsilon_{fat}^{\sigma} + \varepsilon_{fat}^{COD}$, can be added either immediately after the application of the cycling stress increment or they can be introduced into the model in the unloaded configuration. The latter approach proved to be more robust from the numerical point of view, and thus it was used in the examples presented in this paper. This approach is clearly visible in Fig. 5. In this figure the fatigue damage is introduced into the model at each material point in the unloaded configuration. This results in the reduced stiffness during the subsequent reloading and also reduced maximal load carrying capacity.

For the damage calculation, additional state variables are included in the model: σ_{bas} - stress level before the cycling loading, w_{bas} - crack opening displacement before the cycling loading, N - number of load cycles to failure and ε_{fat}^{f} - total contribution to the maximal fracturing strain $\varepsilon_{\max}^{f}$ from fatigue.

3. Validation Example

The presented model is validated using experimental data by Kessler-Kramer [7]. This experiment represents a high-cyclic tensile test at various load levels. The details about the tests are described in the thesis. Section 3.5.2.4. contains the description and experimental results of the analysed specimen. Its geometry is shown in Fig. 2a. It is a prism with cross-sectional area 100x100 and two notches with the depth of 20 mm. The numerical finite element model is shown in Fig. 2b. Due to the two vertical planes of symmetry of the test, the finite element model consists of only one quarter of the specimen.

The bottom part of the model is fixed and the loading is applied along the top surface. The cycling load is assumed to start from zero up to load levels corresponding to were 0.9, 0.8, 0.7, and 0.6 of the static peak load F_{stat}.

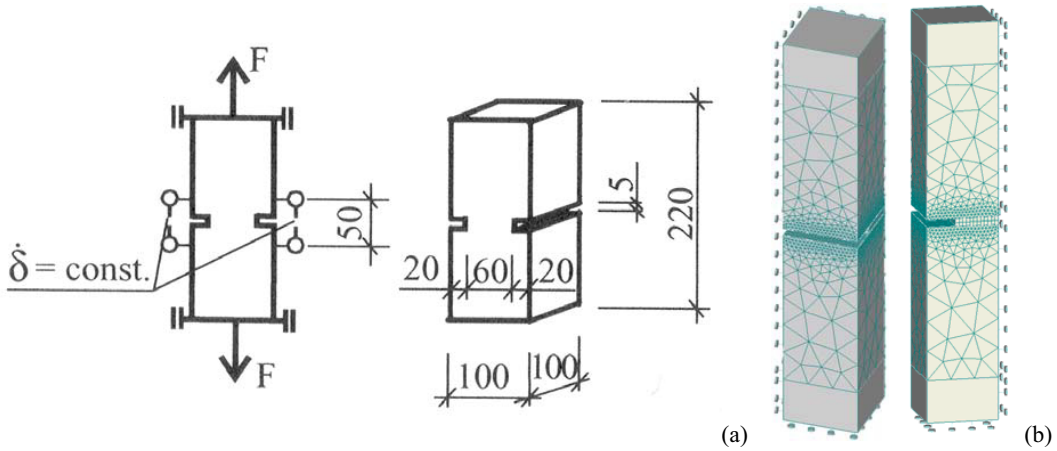

Fig. 2. (a) Validation example geometry [7] (b) finite element mesh.

The parameter β_{fat} was set to 0.052 based on the data measured at load levels 0.7 and 0.9 F_{stat}. The complete material data used in the calculation can be found in **Chyba! Nenalezen zdroj odkazů.**.

Table 1. Material data for NSC-I sealed.

E	μ	f_c	f_t	G_F
[MPa]	[-]	[MPa]	[MPa]	[MN/m]
36 010	0.2	-43.3	3.68	8.878e-5
w_d	ε_{cp}	EXC	FIXED	β_{fat}
[m]	[-]	[-]	[-]	[-]
-5e-4	-1.158e-3	0.52	0.9	0.052

The numerical results are presented in Fig. 3. Note that unlike the physical tests that are carried out until failure, the number of cycles is set before starting the numerical analysis, which then either completes or fails. Therefore,

the analysis does not determine the exact cycle when failure occurs, but that cycle lies between the rightmost empty (completed) and leftmost filled (failed) mark on that particular level.

Besides the exact 0.6, 0.7, 0.8, and 0.9 multiples of the static peak load, the analysis has also been run for load levels decreased by 1.6%. Especially at $0.7\,F_{stat}$, this small load difference results in a significant increase of the number of cycles sustained. Such sensitivity may amplify the effects of sample variations when experiments are carried out, especially considering the sample tested for peak static load is destroyed by the test and can not be subsequently used in the cycling tests with the load levels determined by the static test.

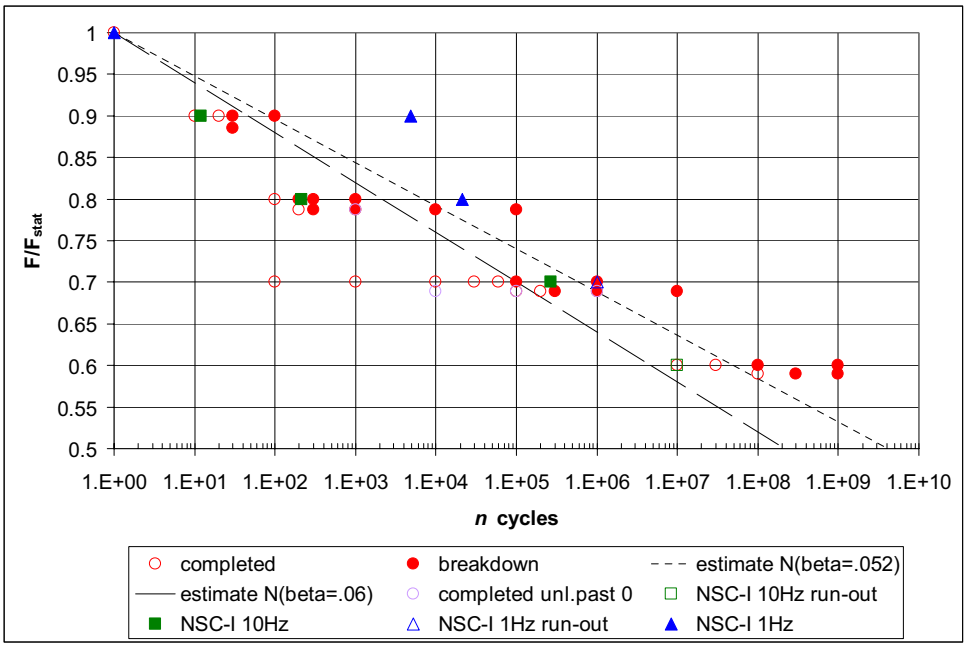

Fig. 3. Numerical results for load levels 0.9, 0.8, 0.7, and 0.6 F_{stat}, β_{fat}=0.052, ξ_{fat}=0.

The samples denoted “completed unl. past 0” were unloaded to a point about 0.1% under 0 before introducing the calculated fatigue damage instead of the 1.6% of F_{stat} above 0, where the unloading of the all other samples was stopped to prevent convergence problems.

The experimental data are denoted by “NSC-I” plus the load frequency 10 Hz respectively 1 Hz. The samples that did not fail (“run-out”) are marked by empty squares respectively triangles.

The numerical results exhibit good agreement with the experimental data at 10 Hz. However, the measured endurance of the samples tested at 1 Hz is much higher, especially for the loads near the static maximal load (0.9 and $0.8\,F_{stat}$) where the slower loading can be sustained for 2-3 orders of magnitude larger number of cycles compared to the 10 Hz and to the numerical results.

For comparison, the “estimate N” lines show the number of cycles resulting from a global application of the S-N curve, i.e., for stress levels calculated by dividing the force by the cross section area of the sample. These lines are included for two values of the β_{fat} parameter, 0.06 and 0.052.

In the analysis, on all the samples that have sustained the applied number of cycles, the load was further increased up to peak to determine the capacity of the damaged sample. The resulting load-displacement diagrams are presented in Fig. 4 along with the results from the static analysis. The results clearly show the effect of the cycling loading. When cycling loading is assumed the model introduces additional damage to the structure. This damage depends on the cycling load level and the number of cycles. This additional cycling damage effects peak load as well as the unloading stiffness of the structure.

Fig. 5 shows in more detail the effect of the fatigue damage. This figure corresponds to the cycling load level of $0.7\,F_{stat}$, 10 000 cycles, β_{fat}=0.052, ξ_{fat}=0. It shows the initial stiffness of the model before the cycling load is applied as well as the structural stiffness after the introduction of the fatigue damage as well as the corresponding peak load. This implies that when 10 000 cycles are considered, the peak load is only about 10% above the cycling load level, however, the final cycling failure occurs when the number of cycles is increased to 100 000 as shown in Fig. 3.

The results for this cycling load level (i.e. $0.7\,F_{stat}$) are studied in more detail in the subsequent figures Fig. 6 to Fig. 8. Fig. 6a shows the expected number of cycles to failure based on the initial stress amplitude at each material point. This figure is shows that in the region very close to the crack tip the expected number of cycles to failure is rather low about 1000 cycles, while the final failure occurred at 10 000 cycles. This is because near the crack tip the stresses are very close to the tensile strength so the fatigue reserve is very low there, but very large further away from the tip. During the cycling load the material points close to the tip fail causing the redistribution of stresses in the structures. When the rest of the structure cannot absorb these redistributed stresses, the fatigue failure occurs. This process is shown in Fig. 6b, Fig. 7 and Fig. 8. Fig. 6a shows the fracturing damage, i.e. fracturing strain ε_{fat}^{f}, which is introduced at each material point as an additional damage due to the cycling loading.

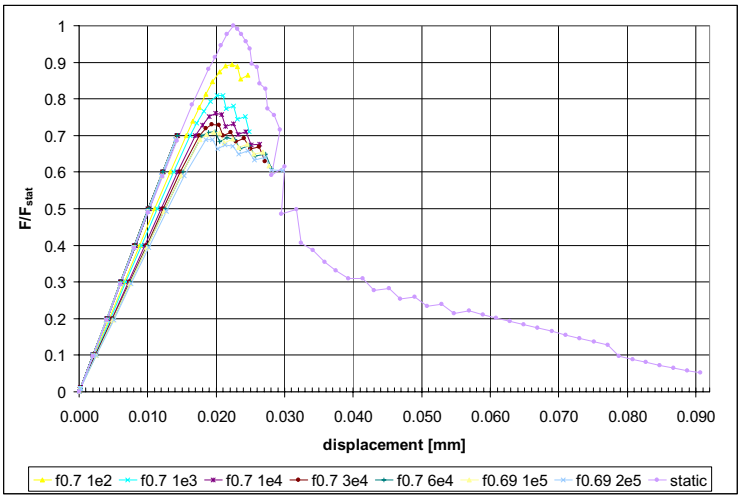

Fig. 4. Numerical L-D diagram for load level $0.7\,F_{stat}$, β_{fat}=0.052, ξ_{fat}=0.

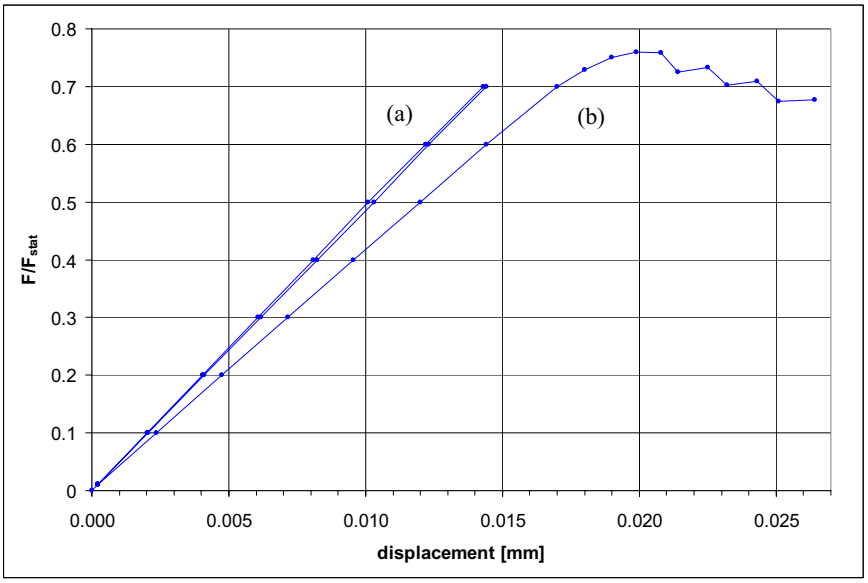

Fig. 5. Numerical load-displacement diagram for 0.7 F_{stat} and 10 000 cycles, (a) before fatigue, (b) after fatigue.

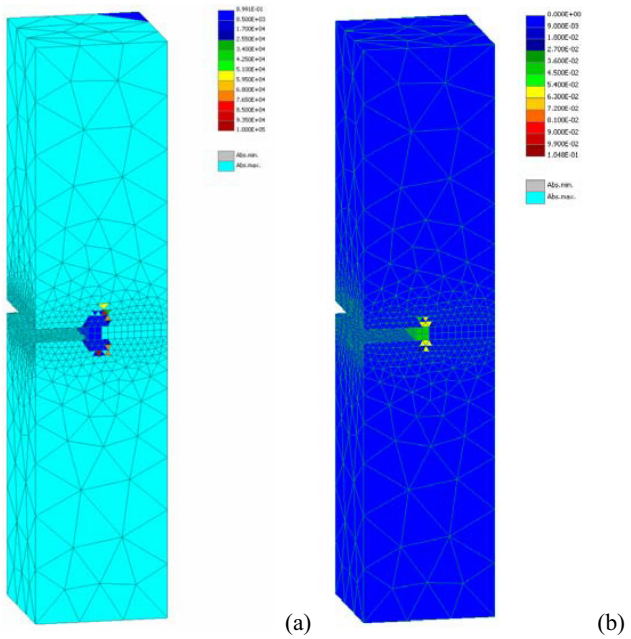

Fig. 6. Cycles to failure (a) and fatigue maximum fracturing strain ε_{fat} (b) for 0.7 F_{stat} and 10 000 cycles

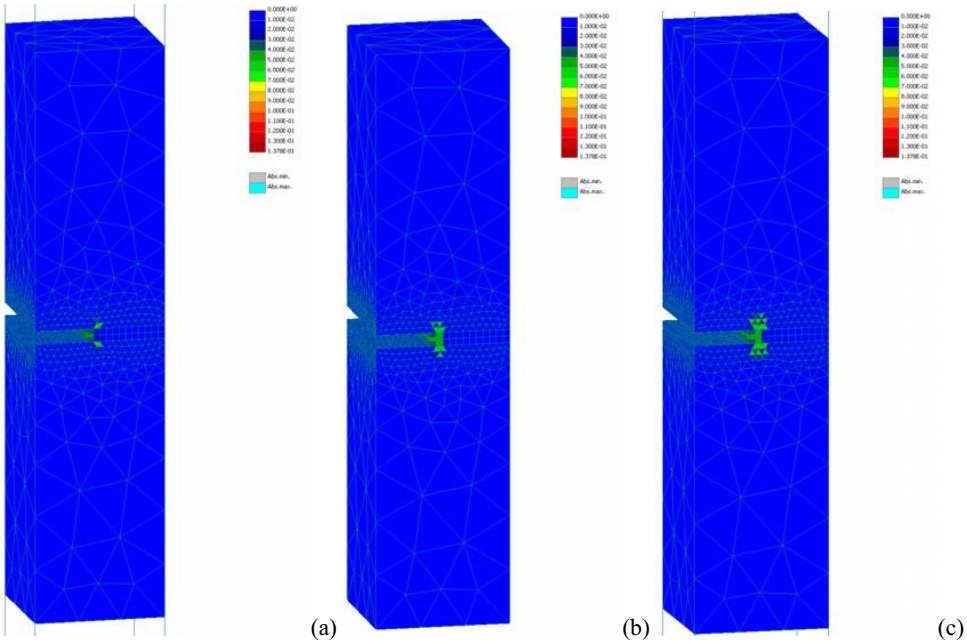

Fig. 7. Fatigue maximum fracturing strain for 0.7 F_{stat} and 1 000 (a), 10 000 (b), and 100 000 (c) cycles

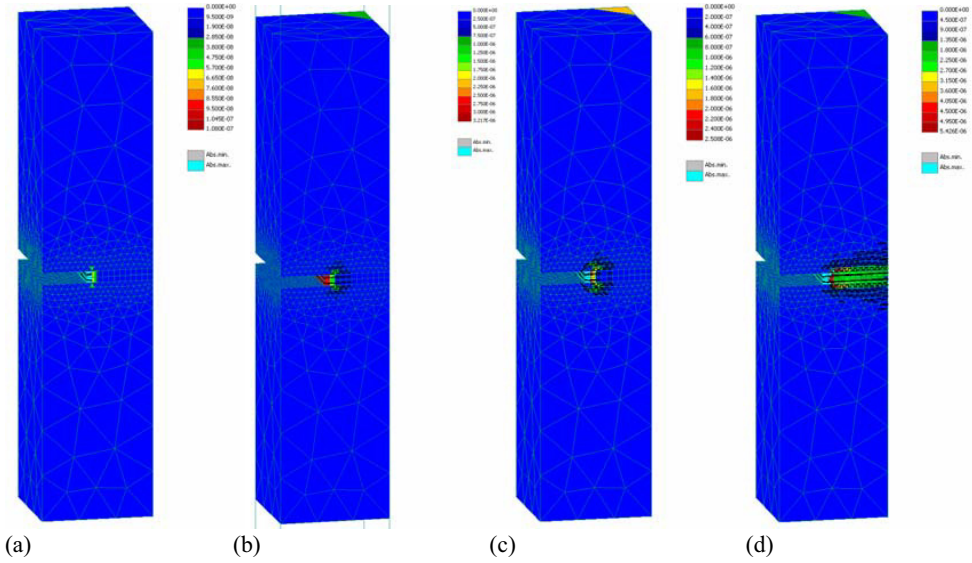

Fig. 8. Crack pattern and crack opening displacement for cycling load level 0.7 F_{stat} and various number of cycles: 1 (a), 1000 (b), 10 000 (c) 100 000 (d) cycles.

Fig. 7 shows the additional fatigue fracturing strain ε_{fat}^{f} for various number of cycles. This fatigue damage is applied at the corresponding material points, which then induces a redistribution of forces and crack propagation. This crack propagation for various numbers of cycles is shown in Fig. 8.

4. Conclusions

A stress based model for fatigue of concrete under tension has been developed and implemented into a finite element program as an extension of an existing three-dimensional fracture-plastic material model [3]. The damage is introduced into the material as maximum reached fracturing strain.

To validate the implementation, an experiment from the literature has been analysed. The numerical results show good agreement with the experimental data. Currently, high-cycle fatigue tests on three-point bending specimens are conducted in Brno [8]. Results from these tests are intended to be used for validation of the numerical model of fatigue material behaviour, parameter calibration, further model development and its improvements.

Acknowledgements

The authors gratefully acknowledge the financial support provide by the Czech Science Foundation under the project No. 103/08/0963 *Basic fatigue characteristic and fracture of advanced building materials*.

References

[1] Hordijk D A. *Local approach to Fatigue of Concrete.* PhD thesis, Delft University of Technology; 1991.
[2] Slowik W, Plizzari G, Saouma, V E. *Fracture of concrete under variable amplitude fatigue loading.* ACI Materials Journal; 1999.
[3] Cervenka J, Papanikolaou V K. *Three Dimensional Combined Fracture – Plastic Material Model for Concrete.* Int. Journal of Plasticity, Volume 24, Issue 12, December 2008, ISSN 0749-6419.
[4] Červenka V, Jendele L, Červenka J. *ATENA Theory Manual.* Cervenka Consulting; 2009.
[5] Červenka J, Jendele L. *ATENA Input File Format.* Cervenka Consulting; 2009.
[6] Fatigue Design Handbook, AE-4, SAE
[7] Kessler-Kramer Ch. *Zugverhalten von Beton unter Ermüdungsbeanspruchung.* Schriftenreihe des Instituts für Massivbau und Baustofftechnologie, Heft 49, Karlsruhe; 2002.
[8] Seitl S, Bílek V, Keršner Z, Řoutil L. Can microsilica improve fatigue behavior of concrete for prestressed elements? In: *Proceedings of FraMCoS-7 (7th International Conference on Fracture Mechanics of Concrete and Concrete Structures)*, IA-FraMCoS; *submited.*